

Deep-Unfolded Joint Activity and Data Detection for Grant-Free Transmission in Cell-Free Systems

Gangle Sun^{1,2}, Wenjin Wang^{1,2}, Wei Xu^{1,2}, and Christoph Studer³

¹*National Mobile Communications Research Laboratory, Southeast University, Nanjing, China*

²*Purple Mountain Laboratories, Nanjing, China*

³*Department of Information Technology and Electrical Engineering, ETH Zurich, Switzerland*
email: sungangle@seu.edu.cn, wangwj@seu.edu.cn, wxu@seu.edu.cn, and studer@ethz.ch

Abstract—Massive grant-free transmission and cell-free wireless communication systems have emerged as pivotal enablers for massive machine-type communication. This paper proposes a deep-unfolding-based joint activity and data detection (DU-JAD) algorithm for massive grant-free transmission in cell-free systems. We first formulate a joint activity and data detection optimization problem, which we solve approximately using forward-backward splitting (FBS). We then apply deep unfolding to FBS to optimize algorithm parameters using machine learning. In order to improve data detection (DD) performance, reduce algorithm complexity, and enhance active user detection (AUD), we employ a momentum strategy, an approximate posterior mean estimator, and a novel soft-output AUD module, respectively. Simulation results confirm the efficacy of DU-JAD for AUD and DD.

Index Terms—Cell-free, deep unfolding, joint activity and data detection, massive machine-type communication.

I. INTRODUCTION

Massive machine-type communication (mMTC) is a core component of fifth-generation (5G) wireless communication systems. mMTC is characterized by intermittent data transmissions from user equipments (UEs) to an infrastructure basestation (BS). Massive grant-free transmission techniques have proven to be effective for mMTC scenarios, as they alleviate signaling overhead, network congestion, and transmission latency by facilitating direct signal transmission from active UEs over shared resource elements, avoiding the need for intricate scheduling mechanisms [1]–[4].

To improve coverage for UEs in mMTC scenarios, cell-free communication has emerged as a powerful solution [5], [6]. Cell-free communication ameliorates inter-cell interference and boosts spectral efficiency through joint processing of

This paper extends our box-constrained FBS algorithm from [1] through deep unfolding, a momentum strategy, an approximate posterior mean estimator, and a novel soft-output AUD module.

This work was supported in part by the National Key R&D Program of China under Grant 2023YFB2904703; in part by the National Natural Science Foundation of China under Grants 62341110, 62371122, and 62022026; in part by the Jiangsu Province Basic Research Project under Grant BK20192002; and in part by the Fundamental Research Funds for the Central Universities under Grants 2242022k30005, 2242022k60002, and 2242023k5003. The work of Gangle Sun was supported in part by the China Scholarship Council under Grant 202206090074.

The authors would like to thank Sueda Taner and Oscar Castañeda for their advice on training deep unfolding networks.

received signals from distributed access points (APs), which interface with a central processing unit (CPU) [2], [7], [8]. For massive grant-free transmission in cell-free systems, crucial tasks encompass active user detection (AUD) and data detection (DD) at the CPU side.

A. Contributions

We propose a deep-unfolding-based joint activity and data detection (DU-JAD) algorithm for massive grant-free transmission in cell-free systems. First, we adapt the box-constrained forward-backward splitting (FBS) algorithm from [1] to approximately solve a joint activity and data detection (JAD) problem, followed by deep-unfolding (DU) its iterations, thereby enabling automated parameter tuning using machine learning. Each unfolded FBS iteration utilizes separate step sizes and a momentum strategy to improve JAD performance. Second, we include an approximate posterior mean estimator (PME) to improve DD. Finally, we propose a new soft-output AUD module that improves user activity detection.

B. Relevant Prior Art

Recent research has concentrated on massive grant-free transmission in cell-free communication systems. References [9] and [10] achieved effective AUD by capitalizing on prominent APs and exchanging activity information between neighboring APs, respectively. Reference [11] focused on the AUD task in asynchronous transmission scenarios. Reference [12] proposed the deep learning-based AUD method to achieve near-real-time transmission. Both [13] and [14] relied on separate AUD and channel estimation (CE) tasks with approximate message passing. Moreover, [2], [15], and [16] explored joint AUD and CE, where [15] proposed individual AP signal processing, [2] addressed quantization artifacts, and [16] utilized channel sparsity in millimeter-wave systems. Reference [17] delved into JAD executed locally at each AP, followed by the culminating joint detection at the CPU based on an adaptive AP selection method. Reference [18] performed joint AUD, CE, and DD through bilinear Gaussian belief propagation, and our previous work in [1] proposed a box-constrained FBS algorithm for these purposes. DU techniques [19] have also gained prominence

$$\mathcal{P}_1 : \left\{ \hat{\mathbf{H}}, \hat{\mathbf{X}}_D \right\} = \arg \min_{\substack{\mathbf{H} \in \mathbb{C}^{MP \times N} \\ \mathbf{X}_D \in \mathcal{B}}} \frac{1}{2} \|\mathbf{Y} - \mathbf{H}[\mathbf{X}_P, \mathbf{X}_D]\|_F^2 + \mu_h \sum_{n=1}^N \sum_{p=1}^P \|\mathbf{h}_{n,p}\|_F + \mu_x \sum_{n=1}^N \|\mathbf{x}_{D,n}\|_F. \quad (7)$$

in this space [16], which combines backpropagation with stochastic gradient descent to optimize algorithm parameters.

In contrast, we focus on JAD for massive grant-free transmission in cell-free systems and propose DU-JAD by utilizing deep unfolding to optimize all algorithm parameters. Furthermore, we include a momentum strategy and an approximate PME, followed by a novel soft-output AUD module that processes the estimated channel and data symbols.

C. Notation

Matrices are denoted by uppercase boldface letters, column vectors by lowercase boldface letters, and sets by uppercase calligraphic letters. The entry at the m th row and n th column of matrix \mathbf{A} is $\mathbf{A}(m, n)$; the m th row vector of matrix \mathbf{A} is $\mathbf{A}(m, :)$. The superscripts $(\cdot)^*$, $(\cdot)^T$, and $(\cdot)^H$ denote conjugate, transpose, and conjugate transpose, respectively; \mathbf{I}_N is the $N \times N$ identity matrix. A diagonal matrix with entries $\{x_1, \dots, x_N\}$ on the main diagonal is $\text{diag}\{x_1, \dots, x_N\}$. The indicator function $\mathbb{I}\{\cdot\}$ is one if its condition is true and zero otherwise. The ℓ_1 norm and Frobenius norm are $\|\cdot\|_1$ and $\|\cdot\|_F$, respectively. The cardinality of the set \mathcal{Q} is $|\mathcal{Q}|$.

II. SYSTEM MODEL AND JAD

We consider a cell-free wireless communication system with frequency-flat and block-fading channels, in which P distributed APs equipped with M antennas each serve N single-antenna UEs. The UEs show sporadic activity, and active UEs occupy R shared resources to transmit their uplink signals.

A. System Model

Following our previous work in [1], the received signals of all APs, $\mathbf{Y} \in \mathbb{C}^{MP \times R}$, can be expressed as follows:

$$\mathbf{Y} = \sum_{n=1}^N \xi_n \mathbf{h}_n \bar{\mathbf{x}}_n^T + \mathbf{N} = \mathbf{H}\mathbf{X} + \mathbf{N}. \quad (1)$$

Here, $\xi_n \in \{0, 1\}$ is the activity indicator of the n th UE with $\xi_n = 1$ indicating active state and 0 otherwise. The channel vector between APs and the n th UE is $\mathbf{h}_n = [\mathbf{h}_{n,1}^T, \mathbf{h}_{n,2}^T, \dots, \mathbf{h}_{n,P}^T]^T \in \mathbb{C}^{MP}$ with $\mathbf{h}_{n,p} \in \mathbb{C}^M$ representing the channel vector between the p th AP and n th UE. The signal vector of the n th UE is $\bar{\mathbf{x}}_n = [\bar{\mathbf{x}}_{P,n}^T, \bar{\mathbf{x}}_{D,n}^T]^T \in \mathbb{C}^R$ with $\bar{\mathbf{x}}_{P,n} \in \mathbb{C}^{R_p}$ and $\bar{\mathbf{x}}_{D,n} \in \mathbb{Q}^{R_d}$ being the pilot and data vectors, respectively. In what follows, we consider quadrature phase shift keying (QPSK) data transmission with constellation set $\mathcal{Q} \triangleq \{x : x = \pm B \pm jB\}$ with $B > 0$. The noise matrix is $\mathbf{N} \in \mathbb{C}^{MP \times R}$ and contains i.i.d. circularly-symmetric complex Gaussian entries with variance $N_0 = 1$. For simplicity, we define an equivalent channel matrix $\mathbf{H} \triangleq [\xi_1 \mathbf{h}_1, \xi_2 \mathbf{h}_2, \dots, \xi_N \mathbf{h}_N] \in \mathbb{C}^{MP \times N}$ and signal matrix $\mathbf{X} \triangleq [\mathbf{X}_P, \mathbf{X}_D] \in \mathbb{C}^{N \times R}$, where $\mathbf{X}_P = [\bar{\mathbf{x}}_{P,1}, \bar{\mathbf{x}}_{P,2}, \dots, \bar{\mathbf{x}}_{P,N}]^T \in \mathbb{C}^{N \times R_p}$ is the non-sparse pilot matrix to ensure full use of known information and $\mathbf{X}_D = [\mathbf{x}_{D,1}, \mathbf{x}_{D,2}, \dots, \mathbf{x}_{D,N}]^T \in \mathcal{Q}$

is the row-sparse data matrix with $\mathbf{x}_{D,n} \triangleq \xi_n \bar{\mathbf{x}}_{D,n}$ and $\mathcal{Q} \triangleq \{\mathbf{X} \in \mathbb{C}^{N \times R_d} : \mathbf{X}(n, :)^T \in \{\mathcal{Q}^{R_d}, \mathbf{0}\}, \forall n\}$. We emphasize that the sporadic user activity and inherent channel sparsity among APs render the matrix \mathbf{H} block-sparse.

B. Problem Formulation

While our primary objective is JAD, a precise estimation of the equivalent channel matrix \mathbf{H} improves JAD performance. Therefore, we formulate the JAD optimization problem for massive grant-free transmission in cell-free systems as in [1]

$$\left\{ \hat{\mathbf{H}}, \hat{\mathbf{X}}_D \right\} = \arg \max_{\substack{\mathbf{H} \in \mathbb{C}^{MP \times N} \\ \mathbf{X}_D \in \mathcal{Q}}} P(\mathbf{Y}|\mathbf{H}, \mathbf{X}_D)P(\mathbf{H})P(\mathbf{X}_D), \quad (2)$$

with

$$P(\mathbf{Y}|\mathbf{H}, \mathbf{X}_D) \propto \exp\left(-\frac{\|\mathbf{Y} - \mathbf{H}[\mathbf{X}_P, \mathbf{X}_D]\|_F^2}{N_0}\right). \quad (3)$$

As in [1] and [7], we leverage the following complex-valued block-Laplace model and complex-valued Laplace model to take the sparsity of \mathbf{H} and \mathbf{X}_D into account:

$$P(\mathbf{H}) \propto \prod_{n=1}^N \prod_{p=1}^P \exp(-2\mu_h \|\mathbf{h}_{n,p}\|_F), \quad (4)$$

$$P(\mathbf{X}_D) \propto \prod_{n=1}^N \exp(-2\mu_x \|\mathbf{x}_{D,n}\|_F), \quad (5)$$

where μ_h and μ_x are parameters that determine the sparsity of \mathbf{H} and \mathbf{X}_D , respectively. The discrete nature \mathbf{X}_D due to the constellation \mathcal{Q} renders \mathcal{P}_1 a discrete-valued optimization problem and a naïve exhaustive search is simply infeasible. To arrive at a computationally manageable optimization problem, we relax the set \mathcal{Q} to its convex hull [7]:

$$\mathcal{B} = \left\{ \sum_{i=1}^{|\mathcal{Q}|} \delta_i \mathbf{X}_i : \mathbf{X}_i \in \mathcal{Q}, \delta_i \geq 0, \forall i; \sum_{i=1}^{|\mathcal{Q}|} \delta_i = 1 \right\}. \quad (6)$$

By inserting the above probability density functions into (2) and by relaxing the constellation set to its convex hull, we obtain the optimization problem \mathcal{P}_1 in (7), which we solve approximately with FBS [20].

C. FBS-based JAD Algorithm

With the definition $\mathbf{S} \triangleq [\mathbf{H}^H, \mathbf{X}_D]^H \in \mathbb{C}^{(MP+R_d) \times N}$, the FBS-based JAD algorithm starts by splitting the objective function in \mathcal{P}_1 into

$$f(\mathbf{S}) = \frac{1}{2} \|\mathbf{Y} - \mathbf{H}[\mathbf{X}_P, \mathbf{X}_D]\|_F^2, \quad (8)$$

$$g(\mathbf{S}) = \mu_h \sum_{n=1}^N \sum_{p=1}^P \|\mathbf{h}_{n,p}\|_F + \mu_x \sum_{n=1}^N \|\mathbf{x}_{D,n}\|_F + \mathcal{X}(\mathbf{X}_D), \quad (9)$$

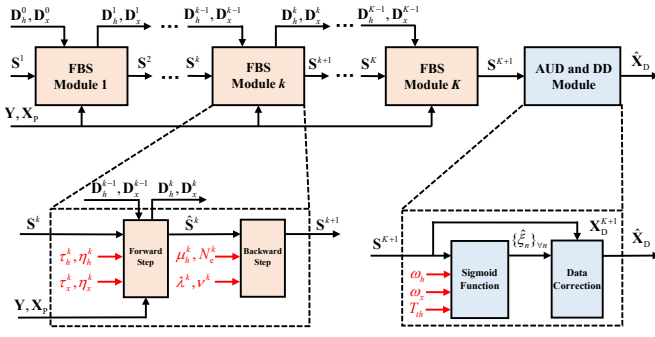


Fig. 1. Architecture of the DU-JAD algorithm.

where $\mathcal{X}(\mathbf{X}_D) = +\infty \mathbb{I}\{\exists \mathbf{X}_D \notin \mathcal{B}\}$ enforces the data to be within the convex set \mathcal{B} . FBS alternates between a gradient-descent step in the smooth function $f(\mathbf{S})$ (the forward step) and performing a proximal operation to find a solution near the minimizer of $g(\mathbf{S})$ (the backward step), where iterations are carried out until a convergence criterion is met. The forward and backward steps are as follows:

1) **Forward Step:** The forward step is given by

$$\hat{\mathbf{S}}^k = \mathbf{S}^k - \tau^k \nabla f(\mathbf{S}^k), \quad (10)$$

where the superscript k indicates the k th iteration, $\hat{\mathbf{S}}^k = [(\hat{\mathbf{H}}^k)^H, \hat{\mathbf{X}}_D^k]^H$, τ^k is the step size [20], and the gradient of $f(\mathbf{S})$ with respect to \mathbf{S} is given by

$$\nabla f(\mathbf{S}) = -[\mathbf{X}^*(\mathbf{Y}^T - \mathbf{X}^T \mathbf{H}^T), \mathbf{H}^T(\mathbf{Y}_D - \mathbf{H} \mathbf{X}_D)^*]^T. \quad (11)$$

2) **Backward Step:** The proximal operator for \mathbf{H} is

$$\mathbf{h}_{n,p}^{k+1} = \frac{\max\left\{\left\|\hat{\mathbf{h}}_{n,p}^k\right\|_F - \tau^k \mu_h, 0\right\} \hat{\mathbf{h}}_{n,p}^k}{\left\|\hat{\mathbf{h}}_{n,p}^k\right\|_F}, \quad (12)$$

and the proximal operation for \mathbf{X}_D involves derivations using the Karush-Kuhn-Tucker conditions; see [1] for the details.

III. DU-JAD: DEEP-UNFOLDING-BASED JOINT ACTIVITY AND DATA DETECTION

Manually tuning the parameters of FBS-based JAD is, in general, tedious. Thus, we apply DU [19], resulting in DU-JAD, which enables automated parameter tuning. DU transforms the iterative procedure of the FBS-based JAD algorithm into a sequential computation process traversing multiple modules with identical structure. The general architecture of DU-JAD is depicted in Fig. 1.

A. FBS Module

1) **Forward Step:** In the forward step of the FBS-based JAD algorithm, the step size τ^k is used when computing $\hat{\mathbf{H}}^k$ and $\hat{\mathbf{X}}_D^k$. Considering the vastly different value ranges of \mathbf{H} and \mathbf{X}_D , we introduce two separate step sizes τ_h^k and τ_x^k in DU-JAD for the computation of $\hat{\mathbf{H}}^k$ and $\hat{\mathbf{X}}_D^k$, respectively. To further accelerate convergence, we include a momentum term

with weights η_h^k and η_x^k . Consequently, the forward step in the k th FBS module of DU-JAD is given by

$$\hat{\mathbf{H}}^k = \mathbf{H}^k + \tau_h^k (\mathbf{Y} - \mathbf{H}^k \mathbf{X}^k) (\mathbf{X}^k)^H + \eta_h^k \mathbf{D}_h^{k-1}, \quad (13)$$

$$\hat{\mathbf{X}}_D^k = \mathbf{X}_D^k + \tau_x^k (\mathbf{Y}_D - \mathbf{H}^k \mathbf{X}_D^k)^H \mathbf{H}^k + \eta_x^k \mathbf{D}_x^{k-1}, \quad (14)$$

where

$$\mathbf{D}_h^k = \tau_h^k (\mathbf{Y} - \mathbf{H}^k \mathbf{X}^k) (\mathbf{X}^k)^H + \eta_h^k \mathbf{D}_h^{k-1}, \quad (15)$$

$$\mathbf{D}_x^k = \tau_x^k (\mathbf{Y}_D - \mathbf{H}^k \mathbf{X}_D^k)^H \mathbf{H}^k + \eta_x^k \mathbf{D}_x^{k-1}, \quad (16)$$

with $\mathbf{D}_h^0 = \mathbf{0}$ and $\mathbf{D}_x^0 = \mathbf{0}$.

2) **Backward Step:** In the backward step of the FBS-based JAD algorithm corresponding to \mathbf{H} , the parameter μ_h is fixed across iterations. To increase flexibility in the FBS-based JAD algorithm, we untie the parameter μ_h as $\{\mu_h^k\}_{\forall k}$ over distinct FBS modules. In the backward step of the FBS-based JAD algorithm corresponding to \mathbf{X}_D , the estimated data matrix may not reside within the set \mathcal{Q} due to relaxation of the discrete set \mathcal{Q} to its convex hull \mathcal{B} . To take into account the discrete nature of the constellation \mathcal{Q} , we propose to use the posterior mean estimation method for DD instead of introducing the penalty term into the objective function as done in [1].

We start by rewriting the n th UE's estimated data vector $\hat{\mathbf{x}}_{D,n}^k$ in the k th iteration as $\hat{\mathbf{x}}_{D,n}^k = \mathbf{x}_{D,n} + \mathbf{e}^k$, where $\mathbf{x}_{D,n}$ is the unknown data vector and \mathbf{e}^k is the estimation error in iteration k . By assuming \mathbf{e}^k follows a complex Gaussian distribution with mean vector $\mathbf{0}$ and covariance matrix $N_e^k \mathbf{I}_{R_D}$, the PME of $\mathbf{x}_{D,n}$ is given by

$$\mathbf{x}_{D,n}^k = \frac{\sum_{\mathbf{x} \in \mathcal{Q}^{R_D}} P_{\text{PME}}^{n,k}(\mathbf{x}) P_a / |\mathcal{Q}^{R_D}| \mathbf{x}}{\sum_{\mathbf{x} \in \mathcal{Q}^{R_D}} P_{\text{PME}}^{n,k}(\mathbf{x}) P_a / |\mathcal{Q}^{R_D}| + P_{\text{PME}}^{n,k}(\mathbf{0})(1 - P_a)}, \quad (17)$$

where P_a represents the user activity probability following $P(\mathbf{X}_D)$, and the function $P_{\text{PME}}^{n,k}(\mathbf{x})$ is defined as

$$P_{\text{PME}}^{n,k}(\mathbf{x}) \triangleq \exp\left(-\frac{\left\|\mathbf{x} - \hat{\mathbf{x}}_{D,n}^k\right\|_F^2}{N_e^k}\right). \quad (18)$$

Evaluating the PME expression of $\mathbf{x}_{D,n}$ incurs high complexity and prone to numerical stability issues. Consequently, we employ an approximate PME as $\mathbf{x}_{D,n}^k = \alpha_n^k \check{\mathbf{x}}_{D,n}^k$. Here, the scaling factor $\alpha_n^k \in [0, 1]$ can be expressed as

$$\alpha_n^k = \min\left\{\frac{1}{\left\|\hat{\mathbf{x}}_{D,n}^k\right\|_1} \max\{\lambda^k \left\|\hat{\mathbf{x}}_{D,n}^k\right\|_1 - \nu^k, 0\}, 1\right\}, \quad (19)$$

where λ^k and ν^k are trainable parameters. Besides, the vector $\check{\mathbf{x}}_{D,n}^k$ is defined as

$$\check{\mathbf{x}}_{D,n}^k \triangleq \frac{\sum_{\mathbf{x} \in \mathcal{Q}^{R_D}} P_{\text{PME}}^{n,k}(\mathbf{x}) \mathbf{x}}{\sum_{\mathbf{x} \in \mathcal{Q}^{R_D}} P_{\text{PME}}^{n,k}(\mathbf{x})}, \quad (20)$$

with the estimation error variance N_e^k to be trained by DU.

B. AUD and DD Modules

To improve AUD, we propose a soft-output module that delivers the probability of each user being active instead of carrying out hard-output decisions. To this end, we propose to use a sigmoid within the AUD module, which leverages the estimated \mathbf{S}^{K+1} to output the likelihood of the user activity status as

$$L_n = \frac{1}{1 + 1/\exp\left(\omega_h \|\mathbf{h}_n^{K+1}\|_F^2 + \omega_x \|\mathbf{x}_{D,n}^{K+1}\|_F^2 - T_{\text{th}}\right)}, \quad (21)$$

with trainable parameters ω_h , ω_x and T_{th} . From the calculated activity probability, the user's active state can be detected by comparing it to a threshold $\bar{L} \in [0, 1]$, i.e.,

$$\hat{\xi}_n = \mathbb{I}\{L_n > \bar{L}\}. \quad (22)$$

As for the DD module, we detect the data matrix as

$$\hat{\mathbf{X}}_D = \text{diag}\{\hat{\xi}_1, \dots, \hat{\xi}_N\} \tilde{\mathbf{X}}_D, \quad (23)$$

where $\tilde{\mathbf{X}}_D = \arg \min_{\mathbf{X} \in \mathbb{Q}^{N \times R_D}} \|\mathbf{X} - \mathbf{X}_D^{K+1}\|_F^2$.

C. Training Procedure

In DU-JAD, the FBS modules and AUD module undergo distinct training processes. For the FBS iterations (equal to the number of modules), we adopt the squared Frobenius norm of the discrepancy between \mathbf{X}_D and \mathbf{X}_D^{K+1} as the loss function for parameter training across K FBS modules, i.e.,

$$\text{Loss}_{\text{FBS}} = \|\mathbf{X}_D^{K+1} - \mathbf{X}_D\|_F^2. \quad (24)$$

For the AUD module's parameter training, we employ the empirical binary cross-entropy (BCE) as the loss:

$$\text{Loss}_{\text{AUD}} = - \sum_{n=1}^N \xi_n \log(L_n) + (1 - \xi_n) \log(1 - L_n). \quad (25)$$

IV. SIMULATION RESULTS

A. System Setup, Performance Metrics, and Baselines

As in [1], we consider a cell-free communication system with $N = 400$ UEs at a height of 1.65 m height and $P = 20$ to 100 APs at a height of 15 m, each with $M = 4$ antennas, all uniformly distributed in a $500 \text{ m} \times 500 \text{ m}$ area. The UE activity $\{\xi_n\}_{\forall n}$ follows an i.i.d. Bernoulli distribution with $P_a = 0.2$. Active UEs transmit $R_p = 50$ pilots, based on a complex equiangular tight frame, and $R_D = 200$ QPSK signals, i.e., $B = \sqrt{0.5}$, over a 20 MHz bandwidth channel at 1.9 GHz. The UEs have 0.1 W transmit power and adhere to a 12 dB power control range. The system works under 8 dB shadow fading variance, 9 dB noise figure, and a 290 K noise temperature. Refer to [1] for more details.

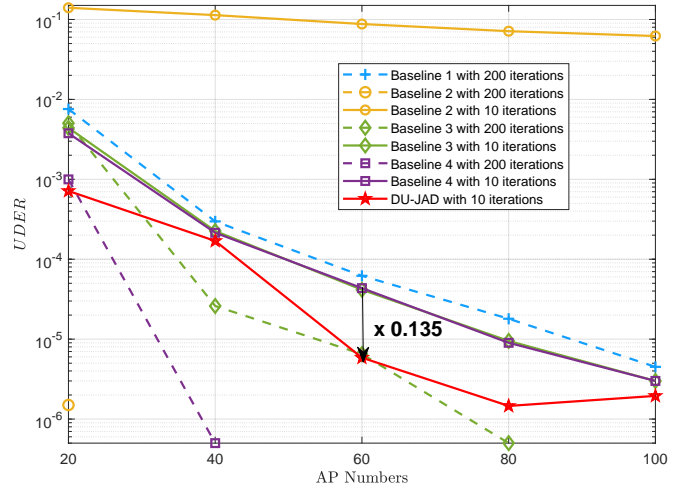


Fig. 2. Active user detection performance.

To evaluate the performance of the proposed DU-JAD, we consider the user detection error rate (UDER) and the average symbol error rate (ASER):

$$\text{UDER} = \frac{1}{N} \sum_{n=1}^N |\xi_n - \hat{\xi}_n|, \quad (26)$$

$$\text{ASER} = \frac{1}{R_D N_a} \sum_{n=1}^N \sum_{r=1}^{R_D} \xi_n \mathbb{I}\{\mathbf{X}_D(n, r) \neq \tilde{\mathbf{X}}_D(n, r)\}. \quad (27)$$

To demonstrate the efficacy of our algorithm, we compare it to the following baselines: “joint AUD-CE via [20], then DD,” “joint AUD-CE via [21], then DD,” “joint AUD-CE-DD via [7],” and “box-constrained FBS algorithm [1],” which are abbreviated as “Baseline 1” through “Baseline 4.” In Baseline 1-4, active UEs are identified by evaluating whether the estimated channel energy, $\|\mathbf{h}_n^{K+1}\|_F^2$, exceeds the threshold T_{AUD} , setting $\hat{\xi}_n$ to 1 if true, and 0 otherwise. Given the estimated channel matrix and active UEs via Baseline 1 and 2, data detection first performs zero-forcing equalization followed by mapping the result to the nearest QPSK symbol. To accelerate convergence, we take the result of the Baseline 1 as the starting point for Baseline 3, Baseline 4 and our DU-JAD algorithm. In DU-JAD, the number of FBS modules is fixed to $K = 10$, while Baseline 1-4 use 200 iterations with a stopping tolerance of 10^{-3} for FBS. For comparison with DU-JAD, we also provide the results of Baseline 2 to 4 with only 10 iterations. In the results shown next, we perform 5000 Monte-Carlo trials.

B. Simulation Results

In Fig. 2, we compare the AUD performance for all considered algorithms. While Baseline 2 with 200 iterations shows the best AUD performance within these methods, its performance drops sharply and becomes the worst when reducing the number of iterations to a more realistic number of 10 iterations. Similarly, Baselines 3 and 4 with 200 iterations yield excellent AUD performance, which significantly deteriorates when running 10 iterations. Compared with these baselines at 10 iterations, the proposed DU-JAD method improves AUD

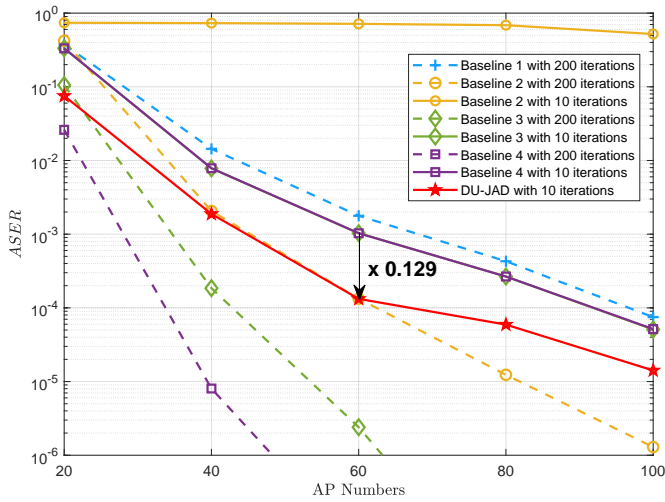


Fig. 3. Data detection performance.

substantially. Notably, the $UDER$ of DU-JAD is only 0.135 of Baseline 3 and 4 at $P = 60$. In addition, it is worth highlighting that the AUD performance of DU-JAD exhibits variability with changes in the number of APs, e.g., its $UDER$ at $P = 100$ is inferior to that at $P = 80$. This variation can be attributed to the AUD module's processing of both estimated channel and data symbols. Since the FBS modules do not include the channel estimation accuracy as an optimization objective, the resulting channel estimates may be inconsistent, which affects the efficacy of the soft-output AUD module.

In Fig. 3, we compare the DD performance for all of these methods. While Baseline 3 and 4 demonstrate better DD performance at 200 iterations, their effectiveness deteriorates if limited to a more practical number of only 10 iterations. At the same time, the performance of Baseline 2 collapses completely when running 10 iterations. Compared to these baselines with 10 iterations, the proposed DU-JAD method significantly improves DD performance. Specifically, the $ASER$ of DU-JAD is only 0.129 of Baseline 3 and 4 at $P = 60$.

V. CONCLUSIONS

We have proposed a novel deep-unfolding-based joint activity and data detection (DU-JAD) algorithm for massive grant-free transmission in cell-free wireless communication systems. When running only 10 algorithm iterations, our proposed DU-JAD method (often significantly) outperforms existing baseline methods in terms of active user detection and data detection performance. This is a result of utilizing deep unfolding, incorporating a momentum strategy, deploying an approximate posterior mean estimator, and using a novel soft-output user activity module.

REFERENCES

[1] G. Sun, M. Cao, W. Wang, W. Xu, and C. Studer, "Joint active user detection, channel estimation, and data detection for massive grant-free transmission in cell-free systems," in *Proc. 24th IEEE Int. Workshop Signal Process. Adv. Wireless Commun. (SPAWC)*, Sept. 2023, pp. 406–410.

[2] M. Ke, Z. Gao, Y. Wu, X. Gao, and K.-K. Wong, "Massive access in cell-free massive MIMO-based Internet of Things: Cloud computing and edge computing paradigms," *IEEE J. Sel. Areas Commun.*, vol. 39, no. 3, pp. 756–772, Mar. 2021.

[3] G. Sun, Y. Li, X. Yi, W. Wang, X. Gao, L. Wang, F. Wei, and Y. Chen, "Massive grant-free OFDMA with timing and frequency offsets," *IEEE Trans. Wireless Commun.*, vol. 21, no. 5, pp. 3365–3380, May 2022.

[4] G. Sun, Y. Li, X. Yi, W. Wang, X. Gao, and L. Wang, "OFDMA based massive grant-free transmission in the presence of timing offset," in *Proc. 13th Int. Conf. Wireless Commun. Signal Process. (WCSP)*, Oct. 2021, pp. 1–6.

[5] A. Mishra, Y. Mao, L. Sanguinetti, and B. Clerckx, "Rate-splitting assisted massive machine-type communications in cell-free massive MIMO," *IEEE Commun. Lett.*, vol. 26, no. 6, pp. 1358–1362, Jun. 2022.

[6] W. Xu, Y. Huang, W. Wang, F. Zhu, and X. Ji, "Toward ubiquitous and intelligent 6G networks: From architecture to technology," *Sci. China Inf. Sci.*, vol. 66, no. 3, p. 130300, Feb. 2023.

[7] H. Song, T. Goldstein, X. You, C. Zhang, O. Tirkkonen, and C. Studer, "Joint channel estimation and data detection in cell-free massive MU-MIMO systems," *IEEE Trans. Wireless Commun.*, vol. 21, no. 6, pp. 4068–4084, Jun. 2022.

[8] W. Xu, Z. Yang, D. W. K. Ng, M. Levorato, Y. C. Eldar, and M. Debbah, "Edge learning for B5G networks with distributed signal processing: Semantic communication, edge computing, and wireless sensing," *IEEE J. Sel. Topics Signal Process.*, vol. 17, no. 1, pp. 9–39, Jan. 2023.

[9] U. K. Ganesan, E. Björnson, and E. G. Larsson, "Clustering-based activity detection algorithms for grant-free random access in cell-free massive MIMO," *IEEE Trans. Wireless Commun.*, vol. 69, no. 11, pp. 7520–7530, Nov. 2021.

[10] X. Shao, X. Chen, D. W. K. Ng, C. Zhong, and Z. Zhang, "Covariance-based cooperative activity detection for massive grant-free random access," in *Proc. IEEE Global Commun. Conf. (GLOBECOM)*, Dec. 2020, pp. 1–6.

[11] Y. Li, Q. Lin, Y.-F. Liu, B. Ai, and Y.-C. Wu, "Asynchronous activity detection for cell-free massive MIMO: From centralized to distributed algorithms," *IEEE Trans. Wireless Commun.*, vol. 22, no. 4, pp. 2477–2492, Apr. 2023.

[12] L. Diao, H. Wang, J. Li, P. Zhu, D. Wang, and X. You, "A scalable deep-learning-based active user detection approach for SEU-assisted cell-free massive MIMO systems," *IEEE Internet Things J.*, vol. 10, no. 22, pp. 19666–19680, Nov. 2023.

[13] S. Jiang, J. Dang, Z. Zhang, L. Wu, B. Zhu, and L. Wang, "EM-AMP-based joint active user detection and channel estimation in cell-free system," *IEEE Syst. J.*, vol. 17, no. 3, pp. 4026–4037, Sep. 2023.

[14] X. Wang, A. Ashikhmin, Z. Dong, and C. Zhai, "Two-stage channel estimation approach for cell-free IoT with massive random access," *IEEE J. Sel. Areas Commun.*, vol. 40, no. 5, pp. 1428–1440, May 2022.

[15] M. Guo and M. C. Gursoy, "Joint activity detection and channel estimation in cell-free massive MIMO networks with massive connectivity," *IEEE Trans. Commun.*, vol. 70, no. 1, pp. 317–331, Jan. 2022.

[16] J. Johnston and X. Wang, "Model-based deep learning for joint activity detection and channel estimation in massive and sporadic connectivity," *IEEE Trans. Wireless Commun.*, vol. 21, no. 11, pp. 9806–9817, Nov. 2022.

[17] R. B. Di Renna and R. C. de Lamare, "Adaptive LLR-based APs selection for grant-free random access in cell-free massive MIMO," in *Proc. IEEE Global Commun. Conf. Workshops (GLOBECOM Workshops)*, Dec. 2022, pp. 196–201.

[18] H. Imori, T. Takahashi, K. Ishibashi, G. T. F. de Abreu, and W. Yu, "Grant-free access via bilinear inference for cell-free MIMO with low-coherence pilots," *IEEE Trans. Wireless Commun.*, vol. 20, no. 11, pp. 7694–7710, Nov. 2021.

[19] A. Balatsoukas-Stimming and C. Studer, "Deep unfolding for communications systems: A survey and some new directions," in *Proc. IEEE Int. Workshop Signal Process. Syst. (SiPS)*, Oct. 2019, pp. 266–271.

[20] T. Goldstein, C. Studer, and R. Baraniuk, "A field guide to forward-backward splitting with a FASTA implementation," *arXiv preprint: 1411.3406*, Nov. 2014.

[21] Z. Chen, F. Sohrabi, and W. Yu, "Sparse activity detection for massive connectivity," *IEEE Trans. Signal Process.*, vol. 66, no. 7, pp. 1890–1904, Apr. 2018.